Available online at www.sciencedirect.com
SCIENCE DIRECT®
Journal of Power Sources 133 (2004) 312–319
JOURNAL OF POWER SOURCES
www.elsevier.com/locate/jpowsour

Fabrication of all-solid-state electrochemical microcapacitors

Joo-Hwan Sung, Se-Joon Kim, Kun-Hong Lee*

Department of Chemical Engineering, Computer & Electrical Engineering Division, Pohang University of Science and Technology (POSTECH), Pohang 790-784, South Korea

Received 20 November 2003; accepted 6 February 2004

Available online 10 April 2004

Abstract

All-solid-state electrochemical microcapacitors are fabricated using photolithography, electrochemical polymerization and solution casting techniques. Gold microelectrode arrays are fabricated by ultraviolet photolithography and a wet-etching method. Conducting polymers such as polypyrrole (PPy) are potentiostatically synthesized on these microelectrodes. A microcapacitor is made up of 50 parallel-connected pairs of microelectrodes. The width of the microelectrodes and the distance between them are each 50 μm. Two types of polymer electrolytes are applied, defined by the polymer matrix and ion-conducting media. Cell capacitance can be controlled by the total synthesis charge of the conducting polymers and a cell potential of 0.6 V is obtained. The electrochemical performance and charging–discharging mechanisms of all-solid-state microcapacitors are studied by cyclic voltammetry (CV), electrochemical impedance spectroscopy (EIS) and constant-current discharge and the results are compared with those of microcapacitors with liquid electrolyte.

Keywords: Micropower; Electrochemical capacitors; Microcapacitors; Conducting polymers; Photolithography; Electrolytes

1. Introduction

Microelectronic devices are attracting attention due to the fast growth in information technology and biotechnology. Accordingly the development of small-sized batteries that can serve as energy sources for microelectronic devices is becoming important. Progress in semiconductor and circuit-design technologies are accelerating decreases in both the weight and the size of devices, and such miniaturization has also diminished the power demand for device operation. In particular, rapid developments in micro-process and electronic material technologies are accelerating high-precision mechanical devices. Again, the development of new energy sources with appropriate current and power is required.

Micropower sources have been developed since the 1980s [1]. Thin-film batteries have been the main theme in this field, but micro- and nano-technologies such as microelectromechanical systems (MEMS), nanoelectromechanical systems (NEMS), microrobots and implantable medical devices require micropower sources with smaller dimensions and higher power density. Conventional thin-film batteries, which have lateral dimensions greater than 1 cm, cannot satisfy these requirements. Therefore, microscopic power devices have been developed using photolithographic techniques [2,3].

Electrochemical capacitors, also known as supercapacitors, are another type of energy-storage device. Generally, their energy densities are greater than those of electrolytic capacitors, and their densities are superior to those of batteries. That is, the electrochemical properties are located between those of electrolytic capacitors and batteries. Therefore, electrochemical capacitors can be used when high power is required and extension of battery discharge time are necessary [4]. If electrochemical capacitors were miniaturized to micron scale, they could satisfy a variety of micropower demands. Electrochemical microcapacitors are, however, still in the early stages of development [5].

Carbon (active carbon, active carbon fiber and carbon nanotubes), metal oxides (RuO_2, IrO_2) and conducting polymers (polyaniline, polypyrrole, polythiophenes and their derivatives) are widely used as electrode material for electrochemical capacitors [6–8]. Of these, conducting polymers are attractive materials because they are relatively cheap, and have good specific capacitances (100–300 F g^{-1}). Furthermore, they can be accurately synthesized to a submicron scale by electrochemical methods, which is very advantageous to microdevice fabrication. Miniaturized elec-

* Corresponding author. Tel.: +82-54-279-2271; fax: +82-54-279-8298.
E-mail address: ce20047@postech.ac.kr (K.-H. Lee).

0378-7753/$ – see front matter © 2004 Elsevier B.V. All rights reserved.
doi:10.1016/j.jpowsour.2004.02.003

trochemical capacitors based on conducting polymers were initially proposed by Wrighton et al. [9]. Full-cell configurations which can be practically operated have been developed in our laboratory using photolithography and electrochemical polymerization techniques [10]. These devices were based on liquid electrolytes. Due to the leakage problems of liquid electrolytes, their direct application to microdevices is severely limited. Therefore, if micropower is to be integrated into microdevices, all-solid-state configurations are necessary.

This study reports the use of a conducting polymer such as polypyrrole as an electrode material, and polymeric ionic conductors such as PVA–H_3PO_4–H_2O and PAN/$LiCF_3SO_3$-EC/PC as solid electrolytes, to form microcapacitors that are solely made up of solid materials.

2. Experimental

The fabrication procedure for the all-solid-state microcapacitors is shown in Fig. 1. Gold microelectrode arrays were fabricated by ultraviolet photolithography and a wet-etching method. Polypyrrole (PPy), a conducting polymer, was synthesized potentiostatically on the microelectrodes. The polymer electrolytes were then coated on the PPy microelectrodes arrays by the solution-casting method. Cyclic voltammetry (CV), electrochemical impedance spectroscopy (EIS) and constant-current discharge were conducted to evaluate the performance of the microcapacitors.

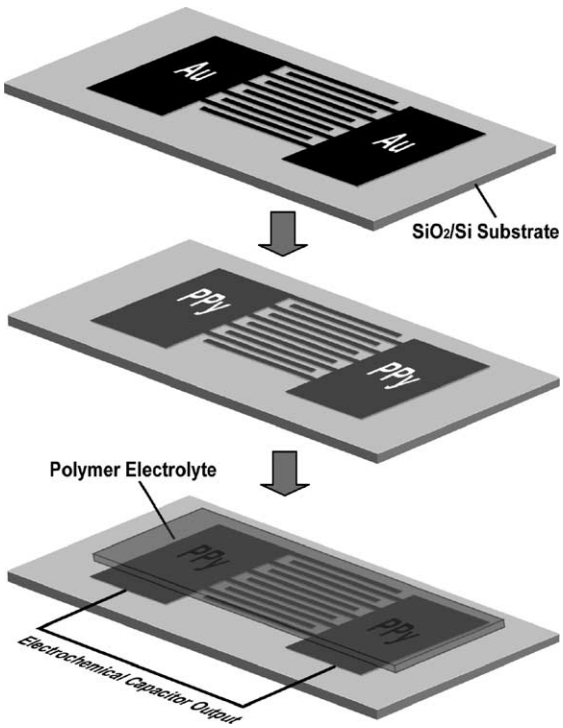

Fig. 1. Fabrication procedure for all-solid-state microcapacitors.

2.1. Fabrication of gold microelectrode and electrosynthesis of conducting polymers

Details of the method used to fabricate the gold microelectrodes have been described in a previous paper [10]. PPy was electrochemically synthesized on the gold microelectrode arrays. A three-electrode set-up was employed—the working electrode was the gold microelectrode array and the counter electrode was a platinum plate. The reference electrode was Ag|AgCl (saturated KCl) or Ag|0.1 M $AgNO_3$($Ag|Ag^+$) according to the electrolyte medium. All electrochemical experiments were performed with an EG&G model 273A potentiostat/galvanostat connected to a personal computer. The PPy was electrosynthesized on the gold microelectrode arrays at 0.65 V versus Ag|AgCl in a 0.1 M pyrrole (Aldrich Chem. Co.) aqueous solution using 0.1 M H_3PO_4 (85%, Kanto Chem. Co. Ind.) as a supporting electrolyte at 25 °C, or at 0.55 V versus Ag/Ag^+ in a 0.1 M pyrrole–propylene carbonate (PC, 99.7%, Aldrich Chem. Co.) solution using 0.2 M lithium triflate ($LiCF_3SO_3$, Tokyo Kasei) as a supporting electrolyte at 25 °C until the desired charges were reached. Water was added (2 vol.%) to the PC solution in order to enhance the electrosynthesis of PPy. The resulting PPy electrodes were maintained in a doping state (as prepared) because in that condition PPy is stable in air. Prior to all experiments, dry N_2 was bubbled through the electrolyte solutions for 30 min, and all electrochemical tests were carried out under dry N_2 atmosphere. All reagents were used without further purification.

2.2. Coating of polymer electrolytes

Two types of polymer electrolyte were examined, the choice depended on the host polymer and ionic conducting media. One was an aqueous-based PVA–H_3PO_4–H_2O gel polymer electrolyte and the other was a non-aqueous-based PAN/$LiCF_3SO_3$-EC/PC gel polymer electrolyte. The PVA electrolytes were synthesized by means of the solution-casting method. PVA powder (Aldrich Chem. Co.) was added to double-distilled water, followed by subsequent heating to 95 °C with vigorous stirring. After the solution became transparent, it was cooled to room temperature and H_3PO_4 was added. The solution was mixed for 12 h in order to obtain a homogeneous solution, and then poured into a Petri dish for evaporation of excess water. When the solution had solidified and in an elastomeric state, it was cut into the proper sizes and firmly attached to the PPy microelectrode arrays.

The manufacturing procedure and conditions for PAN-based gel polymer electrolytes were identical to the method presented in the literature [11]. First, the same weight of EC (ethylene carbonate 99%, Junsei Chem. Co. Ltd.) and PC were mixed, and lithium triflate was added to this solution. Polyacrylonitrile (PAN, Aldrich Chem. Co.) was also added to the solution followed by subsequent heating until a homogeneous solution was obtained. The resulting viscous

solution was then poured on the PPy microelectrode arrays. One or 2 days of gelation time was necessary to obtain a self-sustainable polymer film.

2.3. Electrochemical tests for microcapacitors

Using a frequency response detector (model 1025, EG&G PARC), the ac impedances were measured with an ac signal of 5.0 mV_{rms} at a fixed biased voltage in a two-electrode set-up, in which one electrode was used as the reference and counter electrode and the other as the working electrode. All EIS tests were performed at open-circuit potential (OCP).

3. Results and discussions

Cell codes and preparation conditions for various constructions are summarized in Table 1. The same electrolyte media were used for synthesis and operation because the electrode would be deactivated if different electrolyte was used. Scanning electron microscopy (SEM) images of all-solid-state microcapacitors are presented in Fig. 2. Two adjacent electrodes represent the cathode–anode pair of the microcapacitor. By designing the size of the PPy microelectrodes, the distance between them and the total number of microelectrodes, microcapacitors with various capacities and powers can be easily produced without modifying the fabrication process. The micrographs in Fig. 2 show that PPy films are synthesized on the gold current-collectors, and a PVA-based polymer electrolyte covers the PPy microelectrode arrays. PVA polymer electrolyte seems to be strictly adhered to the PPy electrodes and the SiO_2 substrate. If the contact resistance between the polymer electrolyte and the PPy electrodes is large, electrochemical performance would be worse due to the increase in cell resistance. From the micrographs, it appears that the contact between the two phases is not bad, but it does not mean that there is good contact between the two phases at the molecular level. At the edges of the PPy electrodes, small voids are observed. These are probably formed by the severe contraction of PVA during Pt coating for SEM examination under high vacuum (Fig. 2a and b). The electric field is enhanced at the edge position of an electrode, so that PPys are more easily electrosynthesized than on a flat surface. Therefore, more concentrated and thicker films are formed at the edge position, while flat and uniform films are observed elsewhere (Fig. 2c). As PPy films have higher vertical growth rates than lateral ones, their thickness can be controlled by synthesis charges [10].

3.1. Cyclic voltammetry

Cyclic voltammograms for all-solid microcapacitors made up of PPy electrodes and PVA polymer electrolytes are presented in Fig. 3a. Four different synthesis charges of PPy were applied. Up to 1000 mC, an increase in the synthesis charge of PPy gives rise to higher current output. Above 1000 mC, however, the CV shows somewhat resistor-like behavior and its current output declines rapidly. This non-ideal behavior was also observed in the case of aqueous-electrolyte-microcapacitors in earlier work [10]. The non-ideal behavior seems to be due to the low ionic conductance inside the relatively thick PPy film.

Cyclic voltammograms for PVA cells show the typical capacitive behavior of an electrochemical capacitor due to the symmetrical electrode configuration and the potential-dependent charging behavior. By contrast, CVs for all-solid microcapacitors are more resistor-like. For comparison, the CV behavior of three types of microcapacitor is presented in Fig. 3b. Two microcapacitors that use polymer ionic conductors as electrolytes (PAN1 and PVA2 cells) display very similar shapes and charging currents, while the microcapacitor operated in an aqueous H_3PO_4 electrolyte (Aq2 cell) has a more rectangular, or ideal, shape. The difference between the liquid and the polymer electrolyte cells is attributed to a difference in cell resistance. This resistance is determined by two factors in the microcapacitors examined here. The first factor is the ionic conductivity of the electrolyte. The ionic conductivity of 0.1 M H_3PO_4 solution is 11 mS cm^{-1} and those of the two polymer electrolytes are about 2 mS cm^{-1}. Low ionic conductivity will increase the cell resistance. The second factor is electrolyte wetting within the electrodes. In the case of all-solid microcapacitors, the polymer electrolyte is coated on the PPy microelectrodes after PPy was dried under atmospheric conditions. Therefore, it is difficult for

Table 1
Configuration of microcapacitor cel1s

Cell	Synthesis charge of PPy (mC)	Synthesis conditions of PPy	Electrolyte of microcapacitors
Aq1	100	0.1 M H_3PO_4 + 0.1 M pyrrole (aq.), 0.65 V vs. Ag|AgCl	0.1 M H_3PO_4 Aqueous electrolyte
Aq2	515		
Aq3	975		
Aq4	1460		
PVA1	113	0.1 M H_3PO_4 + 0.1 M pyrrole (aq.), 0.65 V vs. Ag|AgCl	PVA–H_3PO_4–H_2O polymer electolyte
PVA2	481		
PVA3	964		
PVA4	1534		
PANI	489	0.1 M $LiCF_3SO_3$ + 0.1 M pyrrole (in PC), 0.55 V vs. Ag|Ag^+	PAN/$LiCF_3SO_3$-EC/PC polymer e1ectrolyte

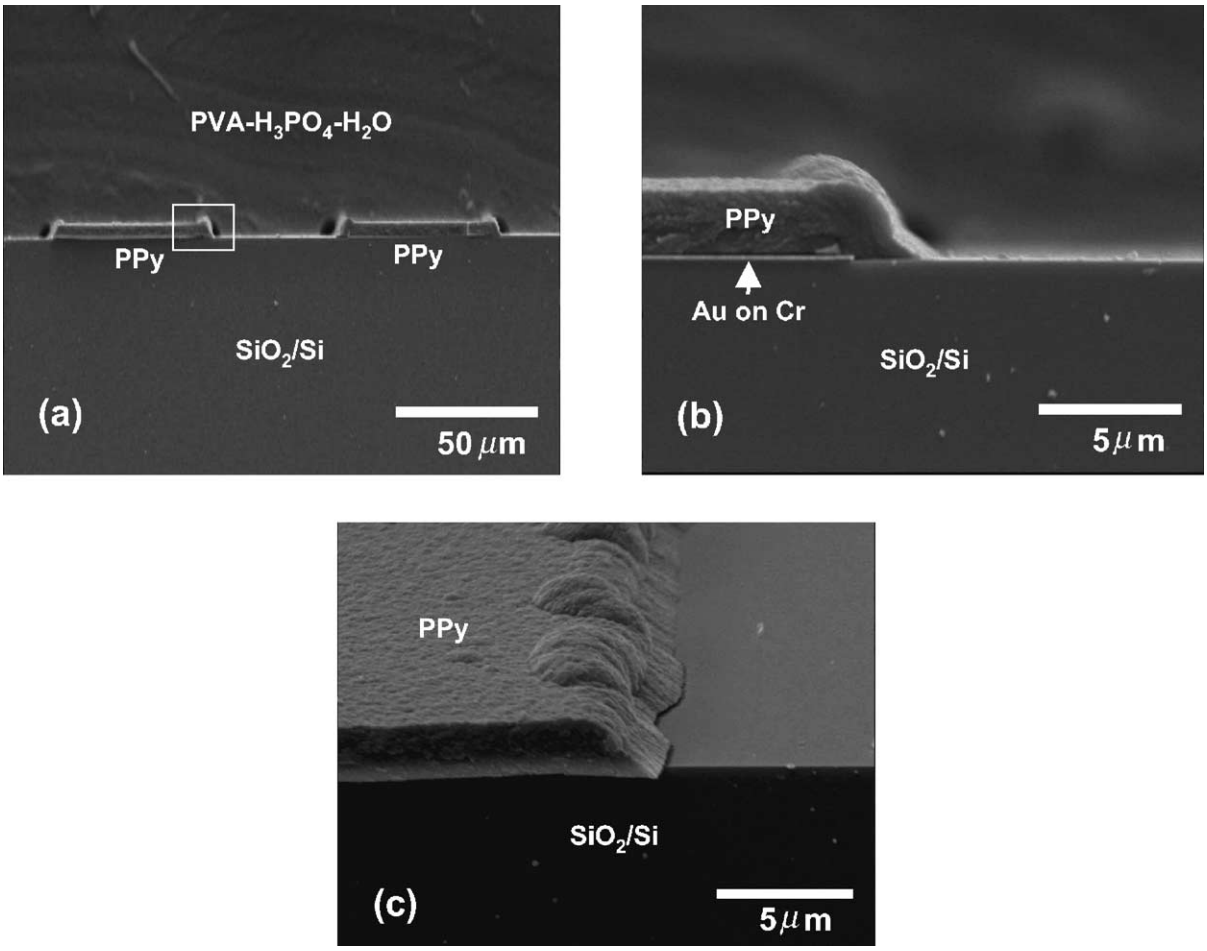

Fig. 2. SEM images of all-solid-state microcapacitors composed of PPy electrodes and PVA–H_3PO_4 electrolytes: (a) and (b) cross-sectional views; (c) slightly tilted view after PVA film is peeled off.

the polymer electrolyte to penetrate deeply inside of the PPy electrodes. As a result, the contact area between the electrode and the electrolyte is restricted on the apparent surface of the PPy electrodes might give rise to the high cell resistance. On the other hand, in the case of the microcapacitors with liquid electrolytes, deep electrolyte wetting inside the PPy electrodes is maintained during cell operation due to the porous PPy structure. Good electrolyte wetting might guarantee the low cell resistance. Considering that the ionic conductivities of three electrolytes are not small, it is considered that the different CV behavior originates mainly from the difference in electrolyte wetting, though this factor together with the above mentioned low ionic conductivity is responsible for the non-ideal CV behavior of all-solid microcapacitors.

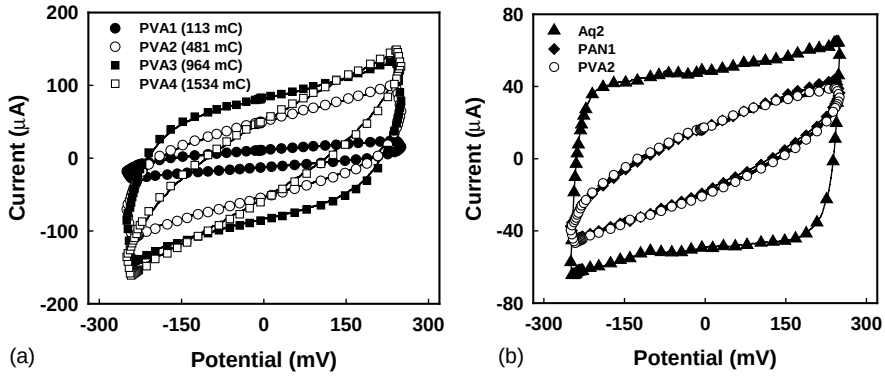

Fig. 3. Cyclic voltammograms for microcapacitors: (a) effect of synthesis charge of PPy; (b) comparison of microcapacitors with three different electrolytes. Obtained with a scan rate of: (a) 50 mV s^{-1} and (b) 10 mV s^{-1}.

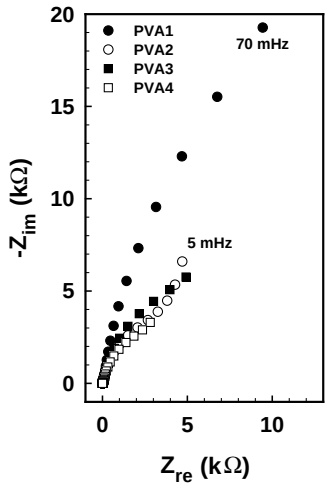

Fig. 4. Nyquist plots for PVA-based microcapacitors.

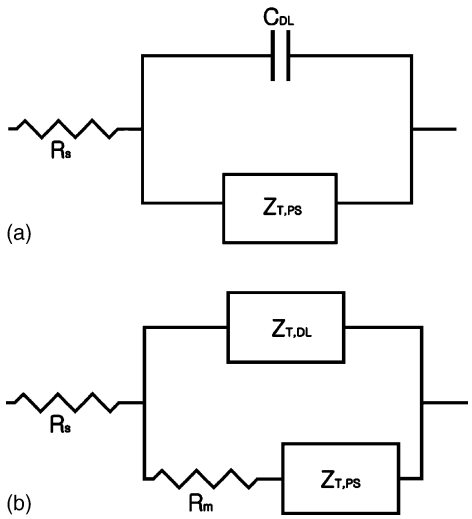

Fig. 5. Equivalent circuits for conducting polymer electrodes: R_s is resistance of electrolyte, C_d is double-layer capacitance, R_m is residual or mixed resistance, and Z is distributed function.

3.2. Electrochemical impedance spectroscopy

Nyquist plots of PVA-based microcapacitor cells are shown in Fig. 4. It is known that a typical Nyquist plot for a conducting polymer has a much declined line at high frequencies and a vertical or slightly declined line at low frequencies if the two axes are set to an identical scale [12,13]. In this study, much declined line up to the very low frequency of 5 mHz are observed. The cell impedances are about one order of magnitude larger than those of aqueous electrolyte microcapacitors [10]. These findings may also be attributed to the lower conductivity of polymer electrolytes and the small wetting areas as stated above, though the much declined line at low frequencies cannot be easily explained. For this reason, an equivalent circuit study was undertaken for the results of impedance spectroscopy.

Various equivalent circuits have been applied to represent the impedance behavior of conducting polymer electrodes [12–15]. Nevertheless, no general equivalent circuit that can satisfy all electrolyte-conducting polymer configurations has been reported. Generally, the circuit in Fig. 5a is applied to a conducting polymer system. It is difficult, however, to represent the full range of impedance behavior with this simple model as it does not give good fitting results for the liquid and the polymer electrolyte systems simultaneously.

It is widely accepted that electric charge is accumulated both by the double-layer and by the pseudo-capacitance for the conducting polymer electrodes [12–15]. Therefore, two transmission line components, to represent the double-layer and the pseudo-capacitance behavior, were examined (Fig. 5b). The frequency-independent component C_d could not describe the complicated impedance behavior of conducting polymers. Conducting polymers have pores, i.e., interchain and/or interparticular voids. Therefore, it is reasonable to consider a conducting polymer electrode as a porous electrode. This fact implies that C_d must be frequency-dependent, and treated as a distributed variable. Therefore, C_d was replaced with $Z_{T,DL}$, which is the transmission line component of a double-layer, i.e., the charge accumulation by a non-faradaic reaction. Another main component is $Z_{T,PS}$, which is the transmission line component of pseudo-capacitance, i.e., the charge accumulation by faradaic reactions. It is assumed that the double-layer and the pseudo-capacitance occur independently. The parameter R_m is the residual resistance or the mixed resistances of various components such as the ionic resistance at the PPy/electrolyte interfaces, etc. [16], and R_s is the solution and electrical contact resistance of an electrochemical cell.

All model-fitting processes were conducted by LEVMW CNLS programs developed by Macdonald [17]. The impedance data for liquid electrolyte microcapacitors is well fitted by the two-component-transmission line model up to 5 mHz. The Nyquist plot for the polymer electrolyte microcapacitors is also well fitted, see Fig. 6. As the Nyquist

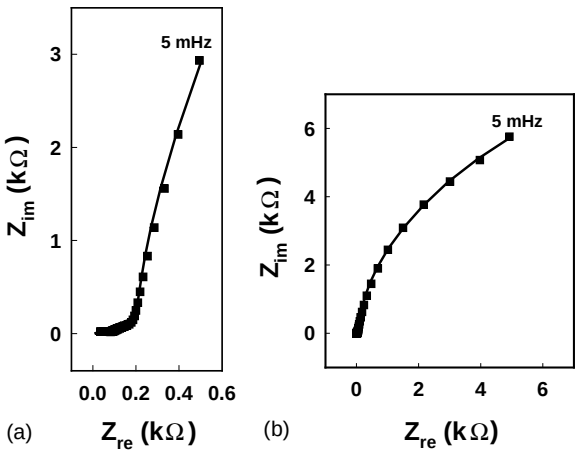

Fig. 6. Comparison of experimental (■) and calculated (—) and Nyquist plots for aqueous and polymer electrolyte microcapacitors. (a) Aq3 cell, (b) PVA3 microcapacitor cell.

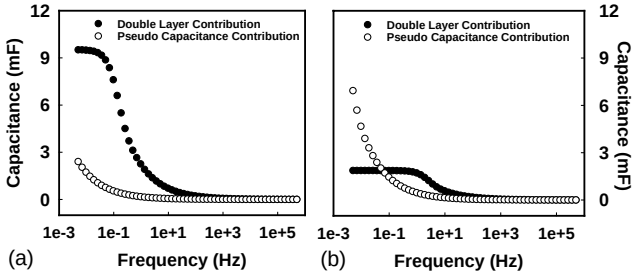

Fig. 7. Contribution of double-layer and pseudo-capacitance to total impedance signals for (a) Aq3 and (b) PVA3 microcapacitor cells.

plots of the two cells are very different, good fitting cannot be obtained with a simple equivalent circuit. Therefore, a somewhat complicated five-parameter model was adopted.

Based on the equivalent circuit model study, the capacitance distributions can be calculated. The results are presented in Fig. 7, in which contribution of the double-layer is separated from that of the pseudo-capacitance. The double-layer capacitance was calculated from the two parameters of $Z_{T,DL}$, as described by the following equation:

$$Z(j\omega) = Z_o \frac{\coth(\sqrt{j\omega\tau})}{\sqrt{j\omega\tau}} \quad (1)$$

where τ is the time constant, and τ and Z_o are the complex parameter that contain system-related parameters such as the diffusion coefficient and the contact area between electrolyte and electrodes [18,19]. This equation describes a porous electrode with the finite-length boundary condition $dc/dx = 0$, which can be formulated with a transmission line that is terminated with an open circuit [20]. Using two fitted parameters, τ and Z_o, the double-layer contribution to the total capacitance can be separated from the impedance signal. Similarly, the pseudo-capacitance contribution, which is due to the faradaic reactions, can be obtained. Basically, double-layer charging–discharging is not a charge-transfer reaction. Therefore, its reaction rate is generally faster than that of a faradaic counterpart; but which reaction is faster is determined by the kinetic parameters of the involved system. Double-layer formation dominates the charging process at high frequencies, while faradaic pseudo-capacitance starts to contribute at low frequencies.

The capacitance dispersions for the two different electrolyte microcapacitors (Aq3 and PVA3 cells) are obviously different (Fig. 7). Aq3 microcapacitors mainly operate by the double-layer mechanism, and the pseudo-capacitance becomes equivalent above 1 kHz. For the polymer electrolyte microcapacitors (PVA3), however, the double-layer contribution is greater than the pseudo-capacitance only from 0.1 up to 100 Hz. The pseudo-capacitance becomes dominant below 1 Hz. The distinguishable difference between two cases appears to be due to electrolyte wetting. As stated above, aqueous electrolyte can wet and penetrate effectively into a PPy electrode, while PPy electrodes are almost dry or solvent-free in a polymer electrolyte cell. If the electrolyte

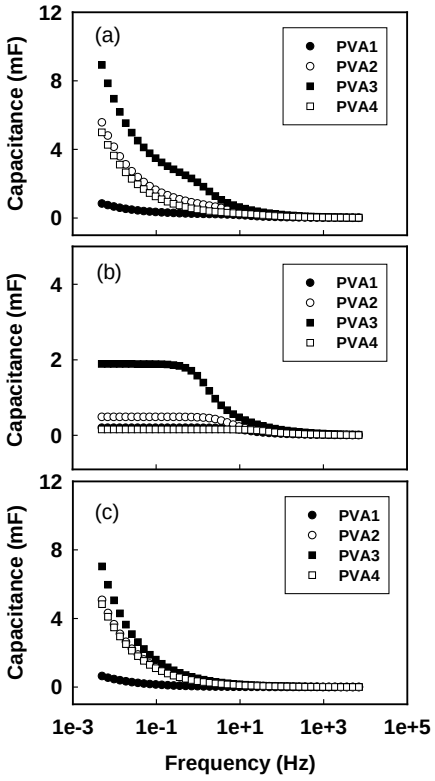

Fig. 8. Effect of synthesis charge of PPy on frequency dispersion of: (a) total capacitance, (b) double-layer capacitance, and (c) pseudo-capacitance.

causes swelling of the conducting polymer electrodes, the double-layer charging would be the main contribution, while an electrode which contains little solvent would be charged mainly by pseudo-capacitance. It seems that the presence of solvent decides which charging mechanism is preferred. It was reported that a double-layer is formed if the electrolytes swell the polymer chain effectively [12,13]. Because there are different points of view regarding the charging mechanism of a conducting polymer electrode, it is assumed here that double-layer and faradic pseudo-capacitance contribute to the electrochemical process simultaneously. Furthermore, both can be represented by a transmission line model with termination at open circuit. Finally, double-layer formation is faster than the pseudo-capacitive faradaic reaction, which is a diffusion-limited slower reaction.

The effects of the synthesis charge of PPy on the capacitance dispersion in the frequency domain are shown in Fig. 8a. Up to 1000 mC (PVA1, PVA2 and PVA3), the increase in the synthesis charge increases the capacitance, while the larger synthesis charge (PVA4) decreases the cell capacitance. Although such a tendency is also observed in CV behavior (Fig. 3.), it can be clearly shown in this impedance plot. For liquid electrolyte microcapacitors, the linear correlation between the capacitance at 5 mHz and the synthesis charge was observed in our previous work [10]. For polymer electrolyte microcapacitors, the highest capacitance value is observed for the PVA3 cell whose

Table 2
Fitting parameters obtained from EIS studies

Sample	R_m	$Z_{T,PS}$ (pseudo)		$Z_{T,DL}$ (double-layer)	
		Z_o	τ	Z_o	τ
Aq1	5.1×10^4	7.9×10^5	4.6×10^2	4.7×10^2	6.0×10^{-1}
Aq2	1.3×10^3	1.2×10^5	3.9×10^2	4.1×10^2	2.3
Aq3	1.4×10^3	4.3×10^5	1.7×10^4	6.1×10^2	5.9
Aq4	1.1×10^3	6.9×10^4	4.4×10^2	6.1×10^2	5.9
PVA1	14.6	3.2×10^5	6.8×10^2	3.1×10^2	6.3×10^{-2}
PVA2	1.6×10^3	3.9×10^5	6.2×10^4	3.2×10^2	1.6×10^{-1}
PVA3	5.0×10^3	1.8×10^5	2.6×10^4	2.7×10^2	5.1×10^{-1}
PVA4	12	2.2×10^5	1.7×10^4	1.2×10^2	1.9×10^{-2}

synthesis charge is 964 mC. A thick PPy electrode appears to diminish the efficiency of active materials. The decrease in capacitance with increasing electroactive material arises from conflicting factors, namely, synthesis charge and ionic and electric conductance. Principally, the capacitance will increase with increasing synthesis charge, which is proportional to the PPy quantity.

The capacitance of the PVA4 cell is smaller than that of the PVA3 cell. The PPy electrodes of polymer electrolyte microcapacitors are little wetted by solvents, thus few ions take part in the electrochemical processes such as double-layer formation and faradaic reaction, and their mobility becomes retarded and the ionic conductance of PPy films is lowered. Actually, the ionic conductivity of PPy that is sufficiently wetted by liquid electrolyte has been reported to be the order of 10^{-5} S cm^{-1} at 0.4 V and 10^{-7} S cm^{-1} at −0.3 V [21]. By contrast, the ionic conductivity of aqueous 0.1 M H_3PO_4 solution is about 10^{-2} S cm^{-1} and that of PVA–H_2O–H_3PO_4 is about 10^{-3} S cm^{-1}. For very thick PPy films, which have synthesis charges of over 1500 mC, the large cell resistance due to the low ionic conductance and the low ion concentration in the film, appears to decrease the cell capacitance even at the low frequencies. The very low ionic conductivity of dry PPy electrodes in PAN and PVA series microcapacitors also seems to be responsible for the smaller capacitance compared with that of aqueous electrolyte microcapacitors.

Double-layer and pseudo-capacitance distributions calculated from transmission line model parameters (Table 2) are presented in Fig. 8b and c, respectively. In all cases, the double-layer capacitance is a minor charging mechanism, its contribution is between 3 and 24%. The highest capacitance for each charging mechanism was obtained with the PVA3 cell. The capacitance dispersion of the double-layer formation fluctuates more than that of the faradaic reaction. This is caused by unstable double-layer formation due to the lack of solvent inside PPy electrodes.

3.3. Constant-current discharge

Constant-current discharge tests were performed under various loads (Fig. 9). The typical discharge behavior of electrochemical capacitors was observed and the cell potentials

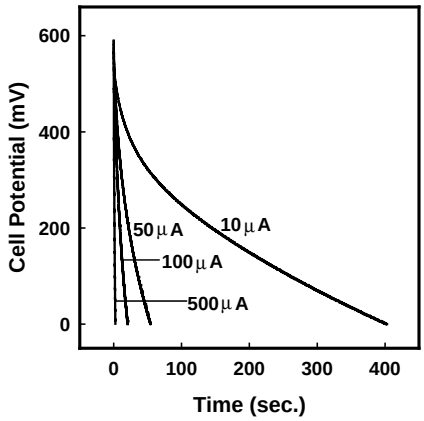

Fig. 9. Constant-current discharge behavior for PVA3 microcapacitor. Current values represent load for each cycle.

were about 0.6 V. Although the microcapacitor cells were charged under 0.6 V, the potential dropped to about 0.5 V on the initial discharge phase. It is thought that low electrolyte conductivity and large electrode resistance caused by the small contact area between the electrode and electrolyte are responsible for the potential drop [22].

4. Concluding remarks

In summary, all-solid electrochemical microcapacitors have been fabricated using photolithography, electrochemical polymerization and solution casting techniques. Gold microelectrodes have been used as the current-collectors and PPy is adopted as the electrode active material. Two types of polymer electrolyte have been investigated for comparison. PVA and PAN have been used as host polymer skeletons and water and PC:EC as conducting media for ionic transportation. Three types of electrochemical test are conducted in order to estimate the performance of all-solid microcapacitors, namely, CV, impedance spectroscopy and constant-current discharge. From an equivalent model study for impedance spectroscopy, the pseudo-capacitance and the double-layer contributions can be separated. For polymer electrolyte cells, the pseudo-capacitance is the main charg-

ing mechanism, whereas double-layer formation contributes primarily to the current output of aqueous electrolyte cells. An increase in the synthesis charge of PPy gives rise to an increase of capacitance up to 1000 mC. On the other hand, the capacitance of the thicker PPy film becomes smaller.

All-solid microcapacitors can be directly integrated into microdevices because they have no electrolyte-leakage problems and their fabrication processes are composed of semi-conductor technologies. Their performance is however, liquid electrolyte configurations. From electrochemical tests, it is concluded that the small contact area between the electrode and the electrolyte, together with low ionic conductance inside the PPy films, deteriorates the electrochemical performance of all-solid microcapacitors. Conducting polymer–polymer electrolyte composite electrodes have been reported [23,24]. According to the literature, the capacity and ionic accessibility are much improved by combining the ionic conducting polymer with electric conducting polymers. These fast-ion conducting electrodes effectively enhance the electrochemical performance of all-solid microcapacitors.

Acknowledgements

This work was supported by the POSRIP and by the BK21 program at Ministry of Education of Korea.

References

[1] K. Kanehori, K. Matsumoto, K. Miyauchi, T. Kudo, Solid State Ionics 9/10 (1983) 1445.
[2] K. Kinoshita, X. Song, J. Kim, M. Inaba, J. Power Sources 81–82 (1999) 170.
[3] L.G. Salmon, R.A. Barksdale, B.R. Beachem, R.M. Lafollette, J.N. Harb, J.D. Holladay, P.H. Humble, in: Proceedings of Solid-State Sensor and Actuator Workshop, 1998, p. 338.
[4] B.E. Conway, Electrochemical Supercapacitors, Kluwer Academic/Plenum Publishers, New York, 1999, pp. 1–31.
[5] J.H. Lim, D.J. Choi, H.K. Kim, W.I. Cho, Y.S. Yoon, J. Electrochem. Soc. 148 (2001) A275.
[6] J.P. Zheng, J. Huang, T.R. Jow, J. Electrochem. Soc. 144 (1997) 2026.
[7] J.P. Zheng, T.R. Jow, J. Electrochem. Soc. 142 (1995) 2699.
[8] S. Panero, E. Spila, B. Scrosati, J. Electroanal. Chem. 396 (1995) 385.
[9] M.S. Wrighton, H.S. White Jr., J.W. Thackeray, US Patent 4,717,673, 1988.
[10] J.-H. Sung, S.-J. Kim, K.-H. Lee, J. Power Sources 124 (2003) 343.
[11] S.S. Sekhon, N. Arora, S.A. Agnihotry, Solid State Ionics 136-137 (2000) 1201.
[12] J. Tanguy, M. Slama, M. Hoclet, J.L. Baudoum, Synth. Met. 28 (1989) C145.
[13] I. Rubinstein, E. Sabatani, J. Rishpon, J. Electrochem. Soc. 134 (1987) 3078.
[14] Y. Li, R. Qian, Synth. Met. 64 (1994) 241.
[15] P. Passiniemi, K. Väkiparta, Synth. Met. 69 (1995) 237.
[16] T. Amemiy, K. Hashimoto, A. Fujishima, Mater. Res. Soc. Symp. Proc. 247 (1992) 613.
[17] www.physics.unc.edu/∼macd/.
[18] B.A. Boukamp, G.A. Wiegers, Solid State Ionics 9/10 (1983) 1193.
[19] I.D. Raistrick, R.A. Huggins, Solid State Ionics 7 (1982) 213.
[20] J.R. Macdonald, Impedance Spectroscopy: Emphasizing Solid Materials and Systems, Wiley, New York, USA, 1987, pp. 59–60.
[21] K. Jüttner, C. Ehrenbeck, J. Solid State Electrochem. 2 (1998) 60.
[22] D. Linden, Handbook of Batteries, McGraw-Hill Inc., New York, USA, 1995, pp. 2.1–2.33.
[23] J. Amanokura, Y. Suzuki, S. Imabayashi, M. Watanabe, J. Electrochem. Soc. 148 (2001) D43.
[24] P. Novák, O. Inganäs, J. Electrochem. Soc. 135 (1988) 2485.